RSC Advances

ROYAL SOCIETY OF CHEMISTRY

www.rsc.org/advances

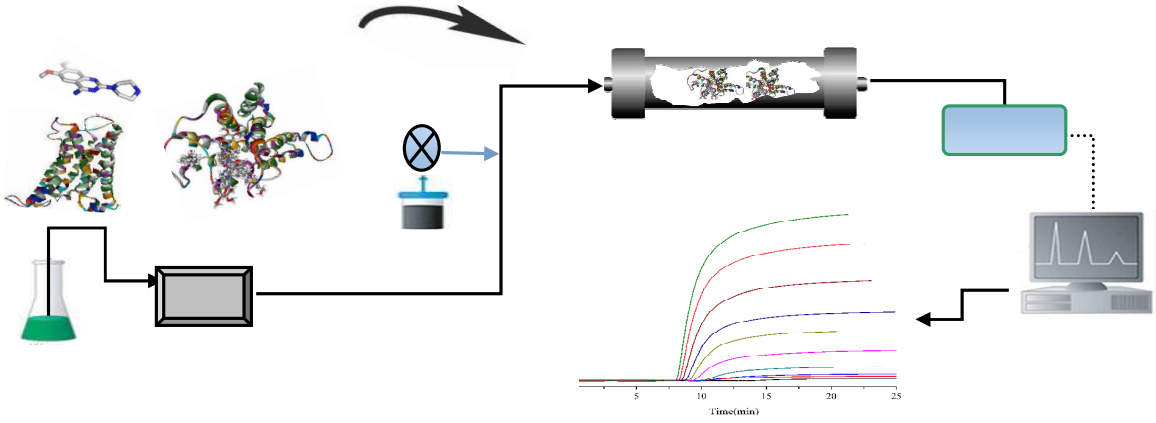

Investigating the binding mechanism of a_{1A}-adrenoceptor and its specific ligands by affinity chromatography.

Journal Name

ARTICLE

Binding mechanism of nine N-phenylpiperazine derivatives and α_{1A}-adrenoceptor using site-directed molecular docking and high performance affinity chromatography

Received 00th January 20xx,
Accepted 00th January 20xx

DOI: 10.1039/x0xx00000x

www.rsc.org/

X. F. Zhao,[a]† J. Wang,[a] G. X. Liu,[a] T. P. Fan,[a,b] Y. J. Zhang,[a] J. Yu,[a] S. X. Wang,[a] Z. J. Li,[c] Y. Y. Zhang[c]† and X. H. Zheng[a]

N-phenylpiperazine derivatives are widely used as clinical drugs for fighting diseases related to cardiovascular system by mediating the signal pathway of α_1-adrenoceptor. The binding mechanism of nine *N*-phenylpiperazine derivatives to α_{1A}-adrenoceptor was explored by molecular docking and high performance affinity chromatography. The methodology involved homology modelling of three dimensional structure of α_{1A}-adrenoceptor, predication of the binding behaviors by LIBDOCK and investigation on the thermodynamic behaviors of the binding by frontal analysis. Molecular docking results showed that Asp[106], Gln[177], Ser[188], Ser[192] and Phe[193] of the receptor were the main binding sites for the nine *N*-phenylpiperazine derivatives binding to α_{1A}-adrenoceptor. The binding was driven by hydrogen bonds formation and electrostatic forces. The affinity of these derivatives to the receptor depended on the functional groups of ionizable piperazine, hydrogen bond acceptor and hydrophobic moiety in the ligand structures. Frontal analysis indicated that association constants of these compounds to the receptor were determined by their structural deviations to the abovementioned functional groups. Thermodynamic studies presented negative enthalpy and Gibbs free energy changes with a positive entropy change, providing proofs that the binding of the derivatives to α_{1A}-adrenoceptor was mainly driven by electrostatic forces. This result was in line with the binding mechanism predicted by molecular docking. It is possible to explore the binding mechanism of drug candidates specifically binding to α_{1A}-adrenoceptor by receptor chromatography.

Introduction

The adrenergic receptors (AR) belong to the family of G-protein coupled seven-transmembrane receptors which serve as the preferable targets for more than fifty percent of approved drugs by U.S. Food and Drug Administration [1-3]. The receptors are divided into three subclasses: α_1, α_2 and β, and further into several subtypes such as α_{1A}, α_{1B}, α_{1D}, α_{2A}, α_{2B}, α_{2C}, β_1, β_2, β_3 [4-7]. Among these subtypes, α_1-ARs play the roles of contracting vascular smooth muscle and human prostate smooth muscle increasing blood pressure, dilating pupil as well as regulating cerebral microcirculation [8]. Regarding these physiological function of α_1-ARs, ligands, especially antagonists of the receptors are introduced to pharmacotherapy and have become the currently first-line medications with considerable success in curing hypertension [9]. In this context, the search for new antagonists of α_1-ARs has attracted great attention in medicinal and analytical chemistry.

A series of techniques have been successfully developed for the pursuit of new ligands binding to known targets. These techniques include computer-aided drug discovery and development [10], high throughput screening assays [11] and fragment-based drug discovery [12]. Another validated strategy for searching new ligands is based on the structure-activity relationship determined by ligand-target interaction analysis. This relationship is further employed to design new candidates with higher affinity and stronger activity to the same target. Modern technologies, videlicet, surface plasmon resonance [13], microdialysis [14] and fluorescence methods [15] have been utilized to explore ligand-target interaction. Affinity chromatography has also proved to be an extremely powerful tool for the same purpose due to the bio-specificity incorporated into the design of the affinity stationary phases and the high specificity, sensitivity and speed of operation resulted from high performance liquid chromatography. Among the affinity chromatographic studies, immobilized human serum albumin is the most widely used stationary phase for revealing the binding of drugs to the protein [16]. More specific stationary phases containing nicotinic acetylcholine receptors [17], P-glycoprotein [18] and cannabinoid (CB1/CB2) receptor [19] are also constructed for the analysis of ligand-protein interaction by attaching the proteins on the surface of solid matrix through physical adsorption or covalent bond.

[a] Key Laboratory of Resource Biology and Biotechnology in Western China, Ministry of Education, College of Life Sciences, Northwest University, Xi'an 710069, China.
[b] Department of Pharmacology, University of Cambridge, Cambridge CB2 1PD, United Kingdom.
[c] Institute of Vascular Medicine, Peking University, Third Hospital and Key Laboratory of Molecular Cardiovascular Sciences, Ministry of Education, Beijing 100083, China.
† Corresponding author: Xinfeng Zhao or Youyi Zhang. E-mail: zhaoxf@nwu.edu.cn (X. Zhao) or zhangyy@bjmu.edu.cn (Y. Zhang)

Our group has found that the stationary phase containing immobilized α_1-ARs has potential in measuring association constant of drug-receptor interaction [20-21]. Despite the capacity to drug-receptor interaction analysis, feasibility of the immobilized α_1-ARs in realizing the binding mechanism of drugs to the receptors needs further investigation.

The antagonists of α_1-AR are claimed with *N*-aryl and *N*-heteroaryl piperazine derivatives [22]. Prazosin, terazosin and doxazosin, the highly selective α_1-AR antagonists, are designed by the use of piperazine-1,4-diyl moiety. The three compounds are the successful cases of improved therapeutic efficacy as a result of subtype selectivity. The structure – affinity activity study of α_1-AR antagonists derived from *N*-phenylpiperazine compounds are continuously necessary in biochemistry, medicine and biology. This work aimed to simulate the interaction between nine *N*-phenylpiperazine derivatives and α_{1A}-AR using site-directed molecular docking. Further work was performed to confirm the validated application of immobilized α_{1A}-AR in analyzing the binding mechanism of these compounds to the receptor by frontal analysis.

Experimental

Materials and instruments

ANTI-FLAG® M1 agarose affinity gel was purchased from Sigma-Aldrich Co. LLC (Saint Louis, MO, USA). Macroporous silica gel (SPS 300-7, pore size 300 Å, particle size 7.0 μm) was from Fuji Silysia Chemical Company Limited (Tokyo, Japan). N-phenylpiperazine derivatives (compounds 1-2, 6-9) were synthesized and identified by the method in our previous report [23]. The purities of these compounds were determined to be more than 98% using high performance liquid chromatography. Standards of doxazosin (Compound 3), prazosin (compound 4) and terazosin (compound 5) were purchased from the Institute of Drug and Biological Product Control of China (Beijing, China). All other reagents were analytically pure unless stated otherwise.

The chromatographic system consisted of an Agilent 1100 series of apparatus including a binary pump, a column oven, a diode array detector (Waldbronn, Germany) and a Chemistation 5.2 software installation for data acquisition and processing. The ZZXT-A type packing instrument was from Dalian Elite Analytical Instruments Co., Ltd (Dalian, China).

Purification and immobilization of α_{1A}-AR

Human embryonic kidney 293 (HEK293) cells stably expressed α_{1A}-AR was prepared and cultured using the method in previous report [24]. The cells were harvested by centrifugation for 10 min with a speed of 3000 rpm at 4 °C. Subsequent treatment was performed by adding three volumes of lysis buffer (50 mM Tris-HCl, 150 mM NaCl, 2 mM DTT, 10% glycerol, pH 7.2) supplemented with a protease inhibitor cocktail (Sigma) to one volume of the obtained cell pellet. The lysate was ruptured in a bead mill for 15 min at 4 °C. Followed by an additional centrifugation for 20 min with a speed of 30,000 rpm at 4 °C, 50 mL of the cell extract was suspended in 5 mM $CaCl_2$ and loaded onto a 5-mL anti-FLAG M1 agarose column. The unbound proteins were removed through eluting the column by loading buffer (20 mM Tris, 500 mM NaCl, 10% glycerol) in the presence of 5 mM $CaCl_2$. Captured proteins were eluted with the loading buffer supplemented with 10 mM EDTA instead of $CaCl_2$. The obtained protein was confirmed to be α_{1A}-AR due to the molecular weight of 66.0 kDa determined by sodium dodecyl sulphate polyacrylamide gel electrophoresis.

The purified α_{1A}-AR was immobilized on the surface of silica gel by a widely reported method [25, 26]. Briefly, γ-aminopropyl triethoxysilane was utilized to convert the hydroxyl group on the gel to amino group, further activated by N, N'-carbonyldiimidazole. The activated gel was suspended in 10.0 mL phosphate buffer (pH = 7.0) in the presence of 4.0 mL α_{1A}-AR for an extra 2.0 h reaction. Rinsed by 150 mL phosphate buffer (50 mM, pH 7.0) containing 2.0 M NaCl, the gel was transferred into 30 mL 1% glycine ethylester solution to remove the residuals of unreacted imidazole group. The immobilized α_{1A}-AR was packed into a stainless steel column (50×4.6 mm, 7.0 μM) using Tris–HCl buffer (5 mM, pH 7.2) as the slurry and propulsive agent under a pressure of 4.0×10^7 Pa.

Molecular docking

Crystal structure of α_{1A}-AR was constructed using homology modelling. In this case, the crystal structure of human β_2-AR (PDB entry: 3SN6) at 2.4 Å resolution [27] was utilized as a template through the search of the related protein structure by BLAST (Basic Local Alignment Search Tool) program [28] in Protein Data Bank database. The amino acidic sequence of the human α_{1A}-AR was retrieved from Swiss-Prot database [29] (accession number P35348, entry name ADA1A_HUMAN) and aligned with human β_2-AR. The three dimensional homology modeling was performed using crystal structural coordinate of template on the basis alignment of target and template sequence of β_2-AR according to the guidelines of Discovery Studio 2.5 (DS 2.5, Accerlrys Software Inc., San Diego, CA). Subsequent structural evaluation was performed by PROCHECK [30] (a program to check the stereochemical quality of protein structures) and PROFILE 3D [31] (a program for the assessment of protein models with three-dimensional profiles). The resulted structure was further optimized through energy minimization before dockings. The structures of the nine *N*-phenylpiperazine derivatives were constructed by DS 2.5 (Fig. 1). The docking study was carried out by LIBDOCK program [32] (site-features docking algorithm), implemented in the software platform of DS. The pose cluster radius was set to 0.5 with top hitss of 10.

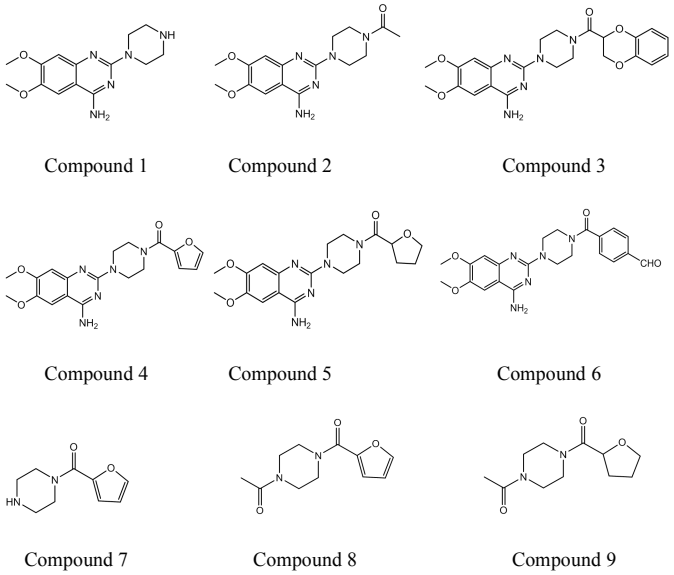

Fig. 1. Chemical structures of nine N-phenylpiperazine derivatives. Compound 1: 2-piperazin-4-amino-6,7-dimethoxy-quinazoline; Compound 2: 1- (4-amino-6,7-dimethoxy-2-quinazolinyl-4- (2-methyl-carbonyl) piperazine; Compound 3: Doxazosin; Compound 4: Prazosin; Compound 5: Terazosin; Compound 6: 1- (4-amino-6,7-dimethoxy-2-quinazolinyl) -4 - [(benzaldehyde 4-yl) carbonyl] piperazine; Compound 7: 1- (2-furoyl carbamoyl) piperazine; Compound 8: 1-acetyl-4- (2-furoyl carbamoyl) piperazine; Compound 9: 1-acetyl-4- (2-tetrahydrofuryl carbamoyl) piperazine

The docking results were characterized by the parameters of inhibition constant, hydrogen bond interaction energy, electrostatic energy, Van der Waal's forces and ligand efficiency. The conformation with the lowest energy was utilized in the docking process.

Frontal analysis

The binding mechanism of *N*-phenylpiperazine derivatives to α_{1A}-AR was secondly analyzed by affinity chromatography using frontal analysis [33]. Capacity factors of each compounds at 20 °C in the initial mobile phase (without addition of any compounds) were calculated by $k' = (t_R-t_0)/t_0$, where k' is the capacity factor; t_R is the retention time of the injection compound; t_0 is the void time of the chromatographic system determined by $NaNO_2$ which is an un-retained solute on the column. The mobile phase was Tris-buffer (5.0 mM, pH 7.2) containing 1.0 mM NaCl and 0.5 mM EDTA. The flow rate was 0.2 mL/min with detection wavelengths of 246 nm for doxazosin, prazosin and terazosin, and 254 nm for the other derivatives.

The association constants of the nine compounds to α_{1A}-AR were determined by frontal analysis. The mobile phases were the solutions containing 0.25, 1.0, 2.0, 4.0, 6.0, 8.0, 12.0, 16.0 and 20.0 μM of each compound prepared using the initial mobile phase. The breakthrough times of each concentration were triply determined to calculate the association constants of each compound to the receptor by Eq. (1):

$$\frac{1}{m_{Lapp}} = \frac{1}{K_A m_L [A]} + \frac{1}{m_L} \quad (1)$$

In this equation, K_A is the association equilibrium constant for the binding of analyte A to the immobilized ligand L, and m_{Lapp} is the apparent moles of analyte required to reach the mean point of a breakthrough curve at a given concentration of applied analyte [A]. According to Eq. (1), the plot of $1/m_{Lapp}$ versus 1/[A] predicts a linear relationship when only one type of binding site is available on the column. The slope and intercept can be used to calculate K_A and the total moles of binding sites m_L for the analyte [34].

Results and discussion

Homology modeling of α_{1A}-AR

The construction of a protein model consists of four steps: sequence alignment between the target and the template; building an initial model; refining the model; evaluating the quality of the model. In this work, these steps were well followed during the construction of α_{1A}-AR homology model. Firstly, a template (3SN6, β_2-adrenergic receptor-Gs protein complex) was identified through homology searches in PDB regarding the sequence identity of 53% to α_{1A}-AR (Supporting information). Ten annotated structures of α_{1A}-AR were predicted among which the desired model was Aalpha.BL00020001 because of the good overlap to the template. This result confirmed by the lowest value of PDF (Probability Density Functions) total energy (-29743.8), PDF physical energy (-5237.6) and DOPE (Discrete Optimized Protein Energy) score (-35692.4) compared with the other models. The ramachandran plot of α_{1A}-AR model calculated by PROCHECK showed that most of the amino acid residues of the receptor distributed in rational region (Supporting information). Further verification of the model by PROFILE 3D showed that 78.4% of the residues had an averaged compatibility of an atomic model (3D) with its own amino acid sequence (1D).

Molecular docking analysis

It is reported that human α_{1A}-AR has 466 amino acids. Two phenylalanine residues (Phe^{208} and Phe^{312}) in transmembrane domain 7 (TM7), one phenylalanine residue (Phe^{193}) in TM5 and one leucine residue in TM6 (Leu^{290}) have been identified as major sites for ligand binding by π-stacking and/or hydrophobic interactions [35-37]. Further experiments of alanine-substitution mutation have showed that two serine residues (Ser^{188} and Ser^{192}) in TM5 played main role in the formation of hydrogen bond between the receptor and ligands [38]. It is also reported that the protonated nitrogen of the bound ligand engages in ionic interactions with an aspartate residue (Asp^{106}) in TM3 [39, 40]. Other mutagenesis studies have indicated that Phe^{86} in TM2 is capable of recognizing the α_{1A}-AR selective antagonist as well as other dihydropyridine-type antagonists. The acidic amino residues Gln^{196}, Ile^{197}, and Asn^{198} in

the second extracellular loop discriminate the α_{1A}-AR selective antagonists (phentolamine and WB4101). Phe^{308} and Phe^{312} in TM7 are major aromatic contacts for most α_1-AR antagonists as well as imidazoline-type agonists.

The overview of the docking complexes of *N*-phenylpiperazine derivatives and α_{1A}-AR was presented in Fig. 2. Asp^{78}, Val^{79}, Cys^{82}, Gln^{149}, Ile^{150}, Ser^{160} and Ser^{164} seemed to play important roles in the drug binding through hydrogen bond formation. The quinazoline and furan system mainly engaged in strong π-stacking and/or hydrophobic interactions with Phe^{58} and Phe^{250}. Other residues including Arg^{68}, Trp^{74}, Tyr^{254}, Trp^{251}, Ser^{55}, Cys^{148}, Trp^{64}, Thr^{146}, Asp^{77}, Ile^{147} and Tyr^{63} participated in ligand binding by Van der Waal's forces. The proposed functional group interaction, especially the binding involving Asp^{78}, Gln^{149}, Ser^{160}, Ser^{164} and Phe^{165} corresponded to the amino acid residues of Asp^{106}, Gln^{177}, Ser^{188}, Ser^{192} and Phe^{193} in previous reports [35]. This means that the specific binding sites for the nine compounds to α_{1A}-AR were consistent with the results of mutagenesis studies [36, 37]. In modelling the interactions of other compounds in this work, we concluded that antagonist binding was docked higher in the pocket than agonist binding, closer to the extracellular surface, and may be skewed toward TM7. This result was consistent with the previous modelling studies where it suggested that the α_{1A}-AR antagonists, prazosin, tamsulosin and KMD-3213 docked with amino acid residues near the extracellular surface.

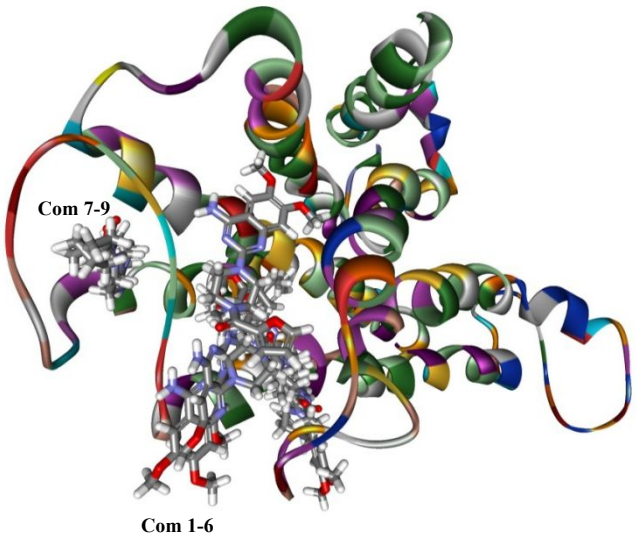

Fig. 2. An overview of the docking complexes of *N*-phenylpiperazine derivatives and α_{1A}-AR. The derivatives were described as sticks. Com 1-6 means compounds 1-6; Com 7-9 presents compounds 7-9.

Purification of α_{1A}-AR

As members of G-protein coupled receptor superfamily, α-ARs have been sub-classified several subtypes on the basis of their relative affinities for variety of ligands. However, little progress has been made in the techniques for their solubilization and purification. In our previous work [26], we have synthesized a new affinity resin f the purification of α-AR by linking the high specific antagonist prazosin, on the surface of agarose gel. It proves that the resin has potential in the purification of native α_1-AR from lysates of cells o animal tissues. In this presentation, we have purified α_{1A}-AR using a commercial anti-FLAG M1 agarose column. Elution of the receptor was accomplished by antibody-mediated affinity chromatography in a calcium-dependent manner.

Compared with the method based on prazosin-derived resin, this mild, calcium-dependent affinity chromatography procedure enabled a rapid purification of α_{1A}-AR. Moreover, the entire purification was accomplished in a single step within several hours, starting from a crude cell homogenate or supernatant, without ever exposing the receptor to conditions other than physiological saline at pH 7.2 (with calcium or EDTA). It was notable that the limitation of the anti-Fl M1 monoclonal antibody ascribed to its specificity only for N terminus of the FLAG fusion protein.

Determination of the association constants by frontal analysis

Affinity chromatography is one of the widely used techniques for exploring drug-protein interaction [41, 42]. This set of experiment aimed to verify the molecular docking predicted mechanism by α_{1A}-AR affinity chromatography using frontal analysis. Representative chromatograms of prazosin by frontal analysis were depicted in Fig.3 when increasing drug concentrations were used in the mobile phases. It was found that each profile of the chromatograms was in good agreement with the shape of sigmoid curve. Same results were also found when the other compounds were applied in the mobile phases. These results indicated that frontal analysis was able to describe the adsorption and disadsorption behaviors of the ni derivatives on the stationary phase containing immobilized α_{1A}-AR.

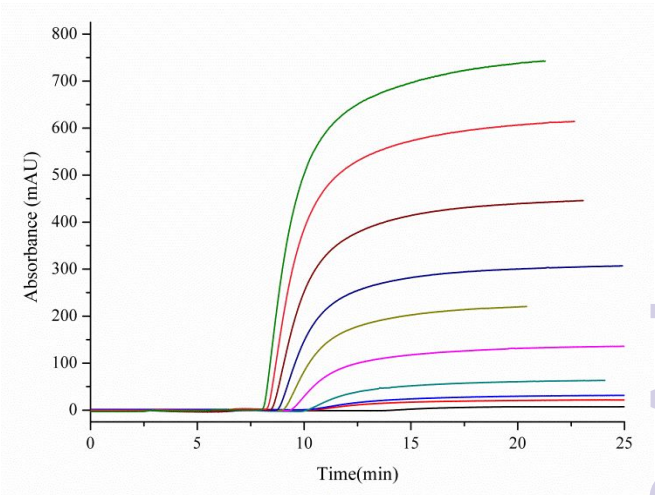

Fig. 3. The representative chromatograms of prazosin by frontal analysis. T concentrations of the drug in the mobile phase were 0.25, 1.0, 2.0, 4.0, 6.0, 8 12.0, 16.0 and 20.0 μM (bottom to top).

The plots obtained for $1/m_{Lapp}$ versus 1/[compound] were depicted in Fig. 4, which gave linear relationships with correlation coefficients ranging from 0.9950 to 0.9993 (Table 1). According to Eq. (1), this result suggested that only a single type of binding site was responsible for the binding of the derivatives on the immobilized α_{1A}-AR. Table 2 summarized the association constants for the compounds to α_{1A}-AR using frontal analysis. The affinity rank order of the nine compounds measured at 20 °C by frontal analysis was compound 3 > compound 4 > compound 6 > compound 5 > compound 2 > compound 1 > compound 7 > compound 8 > compound 9. This order was possible due to the variance of their structural properties.

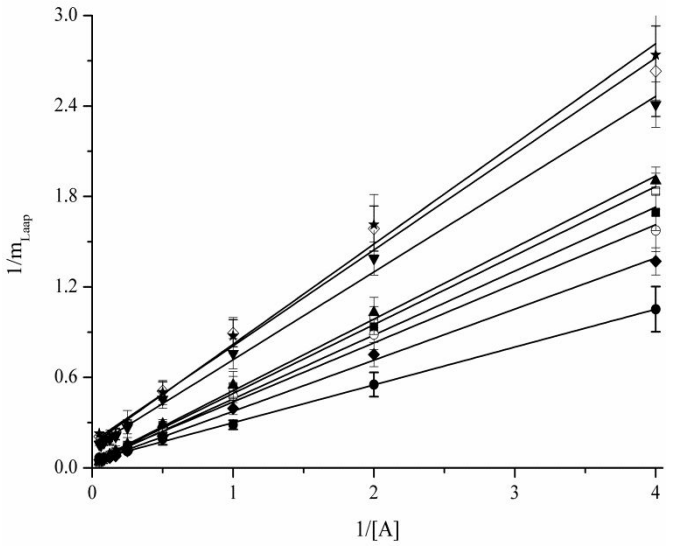

Fig. 4. The plots of $1/m_{Lapp}$ versus 1/[compound] for the nine N-phenylpiperazine derivatives. ■, Compound 1; □, compound 2; ●, compound 3; ○, compound 4; ▲, compound 5; ◆, compound 6; ◇, compound 7; ★, compound 8;▼, compound 9. The experiments were performed at 20 **°C**

Table 1. Regression equations of the curves by plotting $1/m_{Laap}$ versus 1/[A] of the nine *N*-phenylpiperazine derivatives

Compounds	Regression equation	Slope	Intercept	Correlation coefficient
1	$1/mLaap = 0.42\times10^{-6}/[A_{com1}] + 0.031$	0.42	0.031	0.9977
2	$1/mLaap = 0.46\times10^{-6}/[A_{com2}] + 0.035$	0.46	0.035	0.9981
3	$1/mLaap = 0.25\times10^{-6}/[A_{com3}] + 0.048$	0.25	0.048	0.9993
4	$1/mLaap = 0.39\times10^{-6}/[A_{com4}] + 0.046$	0.39	0.046	0.9966
5	$1/mLaap = 0.47\times10^{-6}/[A_{com5}] + 0.037$	0.47	0.037	0.9983
6	$1/mLaap = 0.34\times10^{-6}/[A_{com6}] + 0.036$	0.34	0.036	0.9984
7	$1/mLaap = 0.64\times10^{-6}/[A_{com7}] + 0.017$	0.64	0.017	0.9981
8	$1/mLaap = 0.66\times10^{-6}/[A_{com8}] + 0.015$	0.66	0.015	0.9950
9	$1/mLaap = 0.58\times10^{-6}/[A_{com9}] + 0.013$	0.58	0.013	0.9969

Previous investigation by pharmacophoric model [43] suggested that the three-dimensional structural properties of an ideal α_1-AR antagonist engaged in: a positively ionizable group, corresponding to the more basic nitrogen atom of the aryl piperazine ring; an ortho or meta-substituted phenyl ring, both of which constitutes the arylpiperazine system and satisfy three certain features of the pharmacophoric hypothesis; a polar group that provides a hydrogen bond acceptor feature, filling one of the portions of the pharmacophore that is required at the edge of the molecule opposite to the arylpiperazine moiety; a hydrophobic moiety. The structures of compounds 7-9 only possessed functional group of piperazine group, thus, presented the approximate values of association constants which were far lower than the other six compounds. On the contrary, the structures of compounds 3-6 showed better agreement with these structural properties, as a result, gave the stronger affinity to α_{1A}-AR. Compound 9 presented the weakest affinity to the immobilized α_{1A}-AR due to little accordance with the abovementioned functional groups of ideal α_{1A}-AR ligands.

Focusing on the cases of prazosin and terazosin, the association constants determined by frontal analysis presented good agreements with the data from the literatures under similar experimental conditions [21, 44]. This comparison was rational since Eq. (1) indicates that the determination of association constants by frontal analysis is independent of the number of immobilized protein in column. This indication was possible because the values of the association constants were calculated from the ratio of the intercept to the slope of the equation. This was advantageous for the comparison of K_A values from α_{1A}-AR columns with that from the column having different densities of the receptor. It was also valuable when precise measurement of association constants was required under the conditions that the number of immobilized receptor or the binding capacity of column gradually decreased over the time.

Thermodynamic studies

To verify the binding mechanism of the nine compounds to α_{1A}-AR predicted by molecular docking, the thermodynamic behaviors during the interactions were investigated by affinity chromatography. In this investigation, the bindings of the compounds to α_{1A}-AR were considered to be driven by weak intermolecular forces including hydrogen bonds, Van der Waal's forces, electrostatic forces and hydrophobic interactions. Assuming an identical value for enthalpy change (ΔH^{θ}) during the interaction, calculations of the enthalpy change (ΔH^{θ}), the entropy change (ΔS^{θ}) and the Gibbs' free energy change (ΔG^{θ}) could be followed by eq. (2) and eq. (3):

$$\ln K_a = -\frac{\Delta \mathrm{H}^{\theta}}{RT} + \frac{\Delta S^{\theta}}{R} \quad (2)$$

$$\Delta G^{\theta} = \Delta H^{\theta} - T\Delta S^{\theta} \quad (3)$$

Where ΔH^{θ} and ΔS^{θ} describe the enthalpy and entropy changes accounting for the binding process of the compounds to the receptor, R is the ideal gas law constant and T is the absolute temperature.

Using the semi-empirical law reported by Ross et al [45], the type of the force that drives the binding interaction can be determined by the thermodynamic parameters in eq. (2) and eq. (3).

When ΔH^{θ} >0 and ΔS^{θ} >0, the main force is considered to be hydrophobic interaction. Under the conditions that ΔH^{θ} <0 and ΔS^{θ} >0, electrostatic force is believed to be the main factor pushing the binding. When ΔH^{θ} <0 and ΔS^{θ} <0, hydrogen bonds formation or Van der Waal's force become the main forces during the interaction.

Table 2 listed the association constants of the nine compounds at 10, 20, 30, 37 and 45 °C calculated by eq. (1). It was found that the association constants decreased with growing temperatures, while the number of binding sites gave a positive correspondence to the increasing temperatures. This result was rational because the receptor has at least two conformations at initial time when the column was prepared. Along with the growth of the temperatures, a number of receptors on the rest state changed their conformations to active state, and then served as the binding site for the compounds to α_{1A}-AR. It should be noticed that the capacity factors of the compounds on the immobilized α_{1A}-AR decreased with the increasing temperatures. These results indicated that the retention behavior of the compounds ascribed to the synergistic contribution of the binding site and the association constant. The affinity was the main factor that determined the retention behavior.

Table 2. Calculation of the association constants of the *N*-phenylpiperazine derivatives binding to immobilized α_{1A}-AR

Compounds	Association constants ($\times 10^5$ M^{-1})				
	10 °C	20 °C	30 °C	37 °C	45 °C
1	0.80	0.74	0.66	0.62	0.58
2	0.82	0.76	0.68	0.64	0.59
3	2.04	1.92	1.76	1.68	1.59
4	1.29	1.18	1.05	0.98	0.92
5	0.84	0.79	0.75	0.71	0.68
6	1.12	1.05	0.98	0.95	0.92
7	0.32	0.27	0.23	0.21	0.19
8	0.26	0.23	0.21	0.19	0.18
9	0.25	0.22	0.19	0.17	0.16

The results in Table 2 were further utilized to uncover the relationship between the association constants and the temperatures. As predicated in eq. (2), good linear relationships were obtained between lnK_A and 1000/T for all the compounds in the temperature range (Fig. 5).

As summarized in Table 3, all the compounds gave a principle of $\Delta H^{\theta} < 0$, $\Delta S^{\theta} > 0$ and $\Delta G^{\theta} < 0$, which indicated an endothermic process with an increase of entropy for the interaction. According to the semi-empirical law, the driving force for this process was electrostatic interaction. This result was reasonable because all the compounds were used as the form of amine salts. For instance, prazosin was widely used as prazosin hydrochloride.

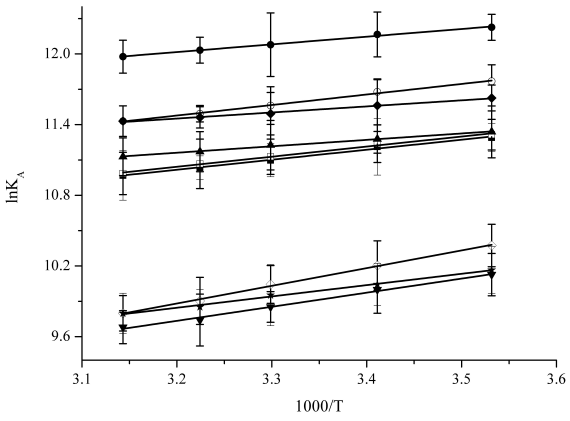

Fig. 5. The plots of lnK_A versus 1000/T for the nine N-phenylpiperaz... derivatives. ■, Compound 1; □, compound 2; ●, compound 3; ○, compound 4; ... compound 5; ◆, compound 6; ◇, compound 7; ★, compound 8; ▼, compound 9

Table 3. Thermodynamic parameters of the N-phenylpiperazine derivative... binding to immobilized α_{1A}-AR calculated at 20 °C.

Compounds	Regression equation	Correlation coefficients	ΔH^{θ} kJ/mol	ΔS^{θ} J/mol·K	ΔG^{θ} kJ/mol
1	$\ln K_A = 848.7/T + 8.30$	0.9950	-7.06±0.24	69.01±2.16	-27.29
2	$\ln K_A = 856.4/T + 8.30$	0.9934	-7.12±0.18	69.01±3.02	-27.35
3	$\ln K_A = 653.7/T + 9.92$	0.9955	-5.43±0.12	82.47±4.18	-29.61
4	$\ln K_A = 893.3/T + 8.62$	0.9966	-7.43±0.31	71.26±1.47	-28.32
5	$\ln K_A = 545.5/T + 9.42$	0.9950	-4.54±0.26	78.32±2.69	-27.50
6	$\ln K_A = 516.1/T + 9.80$	0.9933	-4.29±0.15	81.47±1.94	-28.17
7	$\ln K_A = 1347/T + 5.61$	0.9988	-11.2±0.11	46.64±2.07	-24.8...
8	$\ln K_A = 960.1/T + 6.77$	0.9943	-7.98±0.10	56.29±1.86	-24.48
9	$\ln K_A = 1194/T + 5.91$	0.9937	-9.93±0.22	49.14±2.41	-24.34

Correlation between the fit scores and association constant

In molecular docking, the fit score should give a positive correspondence to the affinity of drug to a receptor. In this point, the K_A values determined by an experimental method are expected to correlate with the docking scores. In this work, the fit scores of the nine compounds were determined to be 93.4 for compound 1, 95.6 for compound 2, 123.2 for compound 3, 117.3 for compound 4, 98.9 for compound 5, 103.8 for compound 6, 87.9 for compound 7, 83.6 for compound 8 and 80.2 for compound 9. The rank order of the scores for the nine compounds binding to α1A-AR was: compound 3 > compound 4 > compound 6 > compound 5 > compound 2 > compound 1 > compound 7 > compound 8 > compound 9. This was in good line with pattern of the association constants by frontal analysis.

To further reveal the relationship between the fit scores by molecular docking and the K_A values by frontal analysis, we plotted the curve of the sores versus the association constants by linear analysis. Th...

result presented a linear relationship between the fit scores and the association constants (Fig. 6). The regression equation was y=23.1x+77.5 with a correlation coefficient of 0.9860. This agreement indicated that the proposed HPAC method will probably become an alternative for exploring drug-receptor binding mechanism.

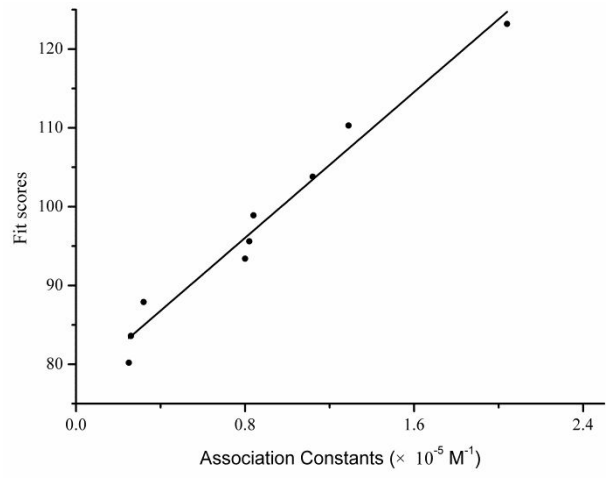

Fig. 6. The plot of the fit scores by molecular docking versus the association constant by frontal analysis

Conclusions

The binding mechanism of nine *N*-phenylpiperazine derivatives to α_{1A}-AR was investigated by molecular docking and frontal analysis. It was found that the binding sites of the nine derivatives to the receptor located at the amino acid residues of Gln^{149}, Phe^{250} Asp^{77} and Ser^{55}. Both molecular docking and thermodynamic investigation by frontal analysis showed that the interaction between *N*-phenylpiperazine derivatives and α_{1A}-AR was driven by electrostatic forces. Molecular docking technique is capable of predicating the mechanism of drug-protein interaction. The immobilized receptor stationary phase has the capacity to realize the drug-receptor binding mechanism and will probably become a powerful methodology for the design and screening of drug candidates specifically binding to a receptor.

Acknowledgements

We appreciated Professor Jiang Ru in Fourth Military University for providing DS software platform and the financial supports from the grant of the National Natural Science Foundation of China (No. 21475103), the Natural Science Foundation of Shaanxi Province (No. 2015JM2072), the program for Innovative Research Team of Shaanxi Province (No. 2013KCT-24) and the Ministry of Science and Technology of the People's Republic of China (No. 2013YQ170525; subproject: 2013YQ17052509)

Notes and references

1 S. Schilit and K.E. Benzeroual, *Clinical Therapeutics*, 2009, **31**, 2489–2502.
2 B.C. Jensen, T.D. O'Connell and P.C. Simpson, *Journal of Molecular and Cellular Cardiology*, 2011, **51**, 518-528.
3 P. Kolb, D.M. Rosenbaum, J.J. Irwin, J.J. Fung, B.K. Kobilka and B.K. Shoichet, *Proceedings of The National Academy of Sciences USA,* 2009, **106**, 6843–6848.
4 I. Nalepa, G. Kreiner, A. Bielawski, K. Rafa-Zablocka and A. Roman, *Pharmacological Reports*, 2013, **65**,1489–1497.
5 J. Hwa, R.M. Graham and D.M. Perez, *The Journal of Biological Chemistry*, 1995, **270**, 23189–23195.
6 S. Cotecchia, Journal of Receptors and Signal Transduction, 2010, **30**, 410–419.
7 J.G. Baker, *British Journal of Pharmacology*, 2010, **160**, 1048–1061.
8 C. Hosoda, T. Koshimizu, A. Tanoue, Y. Nasa, R. Oikawa, T. Tomabechi, S. Fukuda, H. Shinoura, S. Oshikawa, S. Takeo, T. Kitamura, S. Cotecchia and G. Tsujimoto, *Molecular Pharmacology*, 2005, **67**, 912–922.
9 R.M. Graham, D.M. Perez, J. Hwa and M.T. Piascik, *Circulation Research*, 1996, **78**, 737–749.
10 I.M. Kapetanovic, *Chemico-Biological Interactions*, 2008, **171**, 165–176.
11 R. Macarron, M.N. Banks, D. Bojanic, D.J. Burns, D.A. Cirovic, T. Garyantes, D.V.S. Green, R.P. Hertzberg, W.P. Janzen, J.W. Paslay, U. Schopfer and G.S. Sittampalam, *Nature Reviews Drug Discovery*, 2011, **10**, 188-195.
12 C.W. Murray and D.C. Rees, *Nature Chemistry*, 2009, **1**, 187-192.
13 S.G. Patching, *Biochimica et Biophysica Acta*, 2014, **1838**, 43–55.
14 S.J. Sun, C.J. Long, C.Y. Tao, S. Meng and B.Y. Deng, *Analytica Chimica Acta*, 2014, **851**, 37–42.
15 I. Vayá, R. Pérez-Ruiz, V. Lhiaubet-Vallet, M.C. Jiménez and M.A. Miranda, *Chemical Physics Letters*, 2010, **486**, 147-153.
16 R. Matsuda, S.H. Kye, J. Anguizola and D.S. Hage, *Reviews in Analytical Chemistry*, 2014, **33**, 79–94.
17 K. Jozwiak, S. Ravichandran, J.R. Collins and I.W. Wainer, *Journal of medicinal chemistry*, 2004, **47**, 4008–4021.
18 J.Z. Chen and D.S. Hage, *Nature Biotechnology*, 2004, **22**, 1445–1448.
19 R. Moaddel, A. Rosenberg, K. Spelman, J. Frazier, C. Frazier, S. Nocerino, A. Brizzi, C. Mugnaini and I.W. Wainer, *Analytical Biochemistry*, 2011, **412**, 85–91.
20 X.Y. Wang, X. Meng, W.J. Pei, Z.J. Li, Y.Y. Zhang, J.B. Zheng and X.H. Zheng, *Analytical Methods*, 2012, **4**, 3420–3424.
21 X.F. Zhao, H.Y. Lu, J.J. Huang, J.B. Zheng, X.H. Zheng and Y.Y. Zhang, *Chromatographia*, 2012, **75**, 411–415.
22 H. Marona, M. Kubacka, B. Filipek, A. Siwek, M. Dybała, E. Szneler, T. Pociecha, A. Gunia and A.M. Waszkielewicz, *Pharmazie*, 2011, **66**, 733–739.

23 H.F. Wang, Z.L. Zuo, Q.L. Yang, X.J. Shen, X.F. Zhao and X.H. Zheng, *Chinese Journal of Synthetic Chemistry*, 2010, **18**, 745–746.

24 Y. Wang, B.X. Yuan, X.L. Deng, L.C. He, Y.Y. Zhang and Q.D. Han, *Analytical Biochemistry*, 2005, **339**, 198–205.

25 A. Sousa, D. Bicho, C.T. Tomaz, F. Sousa and J.A. Queiroz, *Journal of Chromatography A*, 2011, **1218**, 1701–1706.

26 X.F. Zhao, Q. Li, L.J. Bian, X.H. Zheng, J.B. Zheng, Y.Y. Zhang and Z.J. Li, *Journal of Pharmaceutical and Biomedical Analysis*, 2012, **70**, 549–552.

27 S.G.F. Rasmussen, B.T. deVree, Y.Z. Zou, A.C. Kruse, K.Y. Chung, T.S. Kobilka, F.S. Thian, P.S. Chae, E. Pardon, D. Calinski, J.M. Mathiesen, S.T.A. Shah, J.A. Lyons, M. Caffrey, S.H. Gellman, J. Steyaert, G. Skiniotis, W.I. Weis, R.K. Sunahara and B.K. Kobilka, *Nature*, 2011, **477**, 549–555.

28 A. ʘDriscoll, V. Belogrudov, J. Carroll, K. Kropp, P. Walsh, P. Ghazal and R.D. Sleator, *Journal of Biomedical Informatics*, 2015, **54**, 58–64.

29 R. NaiR and B.Rost. *Protein Science*, 2002, **11**, 2836–2847.

30 R.A. Laskowski, M.W. MacArthur, D.S. Moss and J.M. Thornton, *Journal of Applied Crystallography*, 1993, **26**, 283–291.

31 M.J. Thompson, S.A. Sievers, J. Karanicolas, M.I. Ivanova, D. Baker and D. Eisenberg, *Proceedings of The National Academy of Sciences of The United States of America*, 2006, **103**, 4074–4078.

32 S.N. Rao, M.S. Head, A. Kulkarni and J.M. LaLonde, *Journal of Chemical Information and Modeling*, 2007, **47**, 2159–2171.

33 S. Claesson, *Discussions of the Faraday Society*, 1949, **7**, 34–38.

34 D.S. Hage, A. Jackson, M.R. Sobansky, J.E. Schiel, M.J. Yoo and K.S. Joseph, *Journal of Separation Science*, 2009, **32**, 835–853.

35 L. P. Du and M.Y. Li, *Current Computer-Aided Drug Design*, 2010, **6**, 165-178.

36 D.J. Waugh, R.J. Gaivin, M.J. Zuscik, P. Gonzalez-Cabrera, S.A. Ross, J. Yun and D.M. Perez, *The Journal of biological Chemistry*, 2001, **276**, 25366–25371.

37 J.M. Wetzel, J.A. Salon, J.A. Tamm, C. Forray, D. Craig, H. Nakanishi, W. Cui, P.J. Vaysse, G. Chiu, R.L. Weinshank, P.R. Hartig, T.A. Branchek and C. Gluchowski, *Receptors and Channels*, 1996, **4**, 165–177.

38 D.F. McCune, R.J. Gaivin, B.R. Rorabaugh and D.M. Perez, *Receptors and Channels*, 2004, **10**, 109–116.

39 J. Hwa and D.M. Perez, *The Journal of Biological Chemistry*, 1996, **271**, 6322–6327.

40 D.M. Perez, *Biochemical Pharmacology*, 2007, **73**, 1051–1062.

41 X.F. Zhao, Q. Li, J.J. Chen, C.N. Xiao, L.J. Bian, J.B. Zheng, X.H. Zheng, Z.J. Li and Y.Y. Zhang, *Journal of Chromatography A*, 2014, **1339**, 137–144.

42 X.F. Zhao, Q. Li, C.N. Xiao, Y.J. Zhang, L.J. Bian, J.B. Zheng , X.H. Zheng, Z.J. Li, Y.Y. Zhang and T.P. Fan, *Analytical and Bioanalytical Chemistry*, 2014, **406**, 2975–2985.

43 L. Betti, M. Botta, F. Corelli, M. Floridi, G. Giannaccini, L. Maccari, F. Manetti, G. Strappaghetti, A. Tafi and S. Corsa*Journal of Medicinal Chemistry*, 2002, **45**, 3603–3611.

44 X.K. Gao, Y.Z. Li, Y. Qin, E.H. Chen, Q. Li, X.F. Zhao, L.J Bian, J.B. Zheng, Z.J. Li, Y.Y. Zhang and X.H. Zheng, *RSC Advances*, 2015, **5**, 24449–24454.

45 P.D. Ross and S. Subramanian, *Biochemistry*, 1981, **20**, 3096–3102.